

The Dimensionally Reduced Effective Theory for Quarks in High Temperature QCD

Suzhou Huang*

*Center for Theoretical Physics, Laboratory for Nuclear Science and Department of Physics,
Massachusetts Institute of Technology, Cambridge, Massachusetts 02139;[†]
and Department of Physics, FM-15, University of Washington, Seattle, Washington 98195*

Marcello Lissia[‡]

*Center for Theoretical Physics, Laboratory for Nuclear Science and Department of Physics,
Massachusetts Institute of Technology, Cambridge, Massachusetts 02139;
and Istituto Nazionale di Fisica Nucleare, via Ada Negri 18, I-09127 Cagliari, Italy;[‡]
and Dipartimento di Fisica dell'Università di Cagliari, I-09124 Cagliari, Italy
(November 1995; revised May 1996)*

Abstract

We show that QCD undergoes dimensional reduction at high temperatures also in the quark sector. In the kinematic region relevant to screening physics, where the lowest Matsubara modes are close to their “mass-shells”, all static Green’s functions involving both quarks and gluons, are reproducible in the high- T limit by a renormalizable three dimensional Lagrangian up to order $\tilde{g}^2(T) \sim 1/\ln T$. This three dimensional theory only contains explicitly the lightest bosonic and fermionic Matsubara modes, while the heavier modes correct the tree-level couplings and generate extra local vertices. We also find that the quark degrees of freedom that have been retained in the reduced theory are nonrelativistic in the high- T limit. We then improve our result to order $\tilde{g}^4(T)$ through an explicit nonrelativistic expansion, in the spirit of the heavy quark effective theory. This effective theory is relevant for studying QCD screening phenomena with observables made from quarks, e.g. mesonic and baryonic currents, already at temperatures not much higher than the chiral transition temperature T_c .

I. INTRODUCTION

The behavior of field theories, quantum chromodynamics (QCD) in particular, at finite temperature (T) is of great phenomenological and theoretical interest. In general, we can roughly classify finite temperature physics into two categories: real-time dynamics and screening phenomena. On one hand, real-time dynamics describes the time-dependent response of a system (correlators as functions of real frequency) to time-dependent external probes. On the other hand, screening phenomena refer to the static spatial-dependent response (correlators as functions of the spatial momentum) to time-independent external probes.

Without doubts, real-time dynamics is highly interesting and important, and it could apply, in principle, to a wide range of phenomenological applications. Unfortunately, its complexity and the present lack of systematic nonperturbative approaches make real-time dynamics at finite temperature a territory of field theory that is still, to a very large extent, barely cultivated [1]. In addition, the difficulties of realizing an equilibrated experiment with a given temperature, at least in the specific case of QCD, has practically prevented us from accessing real-time data that are not tempered by some *ad hoc* phenomenological assumptions.

In contrast, the Euclidean nature of the static correlation functions makes the physics associated with screening phenomena relatively simpler. In fact, static correlation functions are determined from equilibrium ensembles and involve no tricky analytic continuation [1,2] and, therefore, screening physics is well-suited to the lattice formulation of field theories at finite temperature. As a consequence, lattice QCD at finite temperature provides us with a large body of measurements not only of bulk quantities, such as the specific heat and pressure, but also of more detailed observables ranging from screening masses [3] to screening wave functions [4].

In the past few years several physical pictures or scenarios have been proposed for properly understanding and interpreting the available lattice data, both the data involving observables made from pure gluonic fields [5] and the data involving observables made from explicit quark fields [6]. One of the most important concepts used in these works is the so-called dimensional reduction (DR) at high temperatures: this concept can be roughly summarized by saying that these QCD screening observables can be effectively described by a three-dimensional theory when temperature is high enough.

The DR picture is based on the observation [7,8] that two different scales appear, in general, in field theories at high T : one scale is order T and the other is order one relative to T (this second scale is strictly order one, i.e. independent of T , only at the tree-level in general). At high T these two scales become vastly separated and certain degrees of freedom effectively decouple; this phenomenon is analogous to the decoupling of heavy particles [9]. So far the existing literature [10–12] has mostly concentrated on situations where the observables involved are purely bosonic: the zero Matsubara modes (scale of order one) are the explicit light degrees of freedom, while the non-zero modes (scale of order T) play the role of the heavy degrees of freedom.

However, we are often interested in observables that couple directly to quark degrees of freedom, observables that would vanish without the explicit presence of quarks in the theory. Our interest in this kind of observables is by no means academic, but rather it is

dictated by the fact that many important observables fall into this class, such as mesonic and baryonic correlators, and in fact such observables have been extensively studied at $T = 0$ [13]. However, less attention has been paid up to now to such correlators between observables made from quark fields in the context of DR. The reason is probably that the scale separation in these situations is less clear, since all fermionic Matsubara modes have energies of order T , due to their antiperiodic boundary condition. Therefore, only the specific underlying dynamics can make DR possible for observables that are made directly with quarks. In other words, it is the theory itself that must generate the scale separation, a necessary condition for the decoupling of some degrees of freedom.

In a recent letter [14] we were able to show in a specific asymptotically free theory, the Gross-Neveu model, that a new scale smaller than T , i.e. $T/\ln T$, naturally emerges at high T . It is this dynamically generated scale that provides the scale hierarchy that in turn makes DR possible for fermionic observables in that model. The purpose of this paper is to examine what happens to QCD at high temperature, to verify that QCD undergoes DR to one-loop order also in the quark sector, and to give the corresponding explicit form of the reduced theory.

As we will show, the DR in the quark sector is not based on the fact that the lightest Matsubara mode (πT) is much lighter than the next lightest mode ($3\pi T$). Instead, the small expansion parameter is the so-called off-shellness or residual momentum after subtracting πT . This expansion parameter roughly measures how far is a given configuration from the noninteracting valence state and its meaning can be clarified by considering the example of the Hydrogen atom. One can usually ignore the two-electron-one-positron configuration relative to the one with a single electron, not because two electrons plus one positron are much heavier than one single electron, but rather due to the fact that the two-electron-one-positron configuration is about 1.5 MeV ($3m_e$) off the energy-shell of the free state, whereas the off-shellness of single-electron configuration is only due to the binding energy, ~ 13 eV.

In the most strict sense DR requires that the reduced theory be renormalizable in three-dimensions and that corrections to correlations calculated in this reduced theory be suppressed by powers of $1/T$.

It is well-known that only the first few terms of the reduced theory are renormalizable in three-dimensions, even when all degrees of freedom are bosonic [11]. In our particular case, we also find a three-dimensional renormalizable Lagrangian only up to one-loop order. Nonetheless, we can still derive an effective theory that is capable of describing screening physics with an accuracy better than the leading order. This kind of reduced theory in general contains higher dimensional operators and needs to be defined in some well-defined regularization scheme. The coefficients of the reduced Lagrangian are determined by requiring that, in the appropriate kinematic regime, the relevant one-particle irreducible graphs calculated in the reduced theory match the corresponding ones in the original theory. It is important to understand that, even though the coefficients are calculated perturbatively, the reduced theory is designed to maintain the infrared properties of the original theory and, hence, the solution of the reduced theory is in general nonperturbative [15].

In the Gross-Neveu model [14] we have explicitly shown that the fermionic degrees of freedom that survive in the reduced Lagrangian are nonrelativistic. Furthermore, it has been suggested [6] that the same happens to the quark degrees of freedom present in the QCD Lagrangian at high T . In this paper, we demonstrate that this is in fact the case

for QCD and hence derive the nonrelativistic Lagrangian for the quarks up to one loop with methods similar to those used in deriving the heavy-quark effective theory [16,17]. This effective Lagrangian should reproduce screening mass splittings up to order $\tilde{g}^4(T)$ and masses themselves up to order $\tilde{g}^2(T)$.

We want to point out from the outset that our effective Lagrangian is relevant for describing the long-distance behavior of spatial correlators only in those channels that are protected by some global symmetry (such as baryon number and flavor) from mixing with gluons, e.g., baryonic and mesonic screening correlators. Furthermore, this reduced theory is not meant for describing correlators that can mix with gluonic state (their large distance behavior is dominated by screening glueball masses), thermodynamical potentials or other bulk quantities that are dominated by the bosonic zero modes. In these later cases, the terms in the effective Lagrangian containing fermions give irrelevant contributions and can be dropped.

The plan of the paper is the following.

In the next section we outline the general strategy and the criteria for dimensional reduction when observables made with quarks are involved. Since the concepts we introduce in Sec. II are somewhat new and cannot be explicitly found in the existing literature, we make the discussion as complete as possible. In particular, we first review the screening physics and the observables the effective theory is intended to describe, e.g. spatial correlators, screening masses and other observables that are identically zero when quarks are explicitly ignored. The relevant kinematic region and the exact meaning of the mass-shell condition in the context of screening physics are specified next. We finally introduce the expansion parameter, the off-shellness, in the same section.

In Sec. III we explicitly calculate the DR Lagrangian, both at the tree and one-loop levels in the specified kinematic region. Composite operators are considered in Sec. IV.

In Sec. V we first discuss a power counting scheme that guarantees that the expansion parameter remains small and, therefore, that the expansion is self-consistent. Then we derive an effective Lagrangian for QCD, where quarks are treated nonrelativistically, in analogy with heavy quarkonium systems. The final form of the reduced Lagrangian and the relationships between parameters in QCD and in the reduced theory are explicitly given. We finally discuss the temperature regime where the reduced theory becomes quantitatively reliable.

The final section contains the summary and our conclusions.

II. GENERAL STRATEGY AND CRITERIA FOR DIMENSIONAL REDUCTION

In this section we set the stage for generalizing the concept of DR to cases that explicitly involve fermions. First we give a brief review of screening physics and an overview of how dimensional reduction comes about: this intuitive guide to our calculation also serves the purpose of introducing an important concept, the “mass-shell” in screening quantities, that is extensively used throughout the paper. Then we state the criterion for DR to take place when observables whose leading contribution comes from fermions are present, after having recapitulated the corresponding criterion for DR in a pure bosonic case. Next we discuss in detail the relevant kinematic regions, relevant to screening physics, where DR could happen

both for fundamental fermionic fields and for composite operators. Finally, we outline the strategy for explicitly verifying whether DR occurs in QCD. Where appropriate we elucidate similarities and differences with the heavy quark expansion.

A. Screening physics and mass-shell condition

Finite temperature screening physics can be directly and naturally formulated in terms of a Lagrangian in the four-dimensional Euclidean space. Unlike real-time dynamics [2], there is no need to eventually analytically continue results to the (3+1)-dimensional Minkowskian space-time, since screening phenomena are described by time-independent correlation functions. Taking advantage of this static nature it is convenient to Fourier transform the fields in the time direction in terms of Matsubara frequencies. Then the four-dimensional Euclidean Lagrangian can be equivalently rewritten as a three-dimensional Euclidean Lagrangian with an infinite number of Matsubara modes.

We typically want to study correlations between operators in the limit of spatial distances much larger than the thermal wavelength, or more specifically, we only consider correlators at $|\mathbf{x}| \gg 1/T$. This large spatial separation selects a preferred direction, which we take along the first axis in the four-dimensional Euclidean space whose zeroth component is the imaginary time. Then the dominant large-distance contributions to such correlators come from the lowest singularities in the external momentum variable p_1 .

If we consider a weakly interacting theory, it is intuitive that singularities appear when the external momentum is such that some of the denominators of the internal propagators vanish. Since the four-momenta are Euclidean and we consider massless particles, denominators are of the form $M^2 + \mathbf{p}^2$ and vanish either when $M^2 = 0$ and $\mathbf{p}^2 = 0$ (bosonic zero mode with vanishing spatial momentum) or when some of the spatial components is imaginary, $p_1^2 = -M^2$ (bosonic non-zero modes $M^2 = (2n\pi T)^2$ and fermionic modes $M^2 = ((2n-1)\pi T)^2$). In this last case p_1 is purely imaginary, which corresponds to an exponentially decaying spatial correlation, a well-expected behavior when only non-zero modes are involved.

In the complex plane of p_1 the condition that the Euclidean four-momentum be zero becomes $(ip_1)^2 - p_2^2 - p_3^2 = M^2$, which can be interpreted as the mass-shell condition in a (2+1)-dimensional Minkowskian space-time for a particle with mass equal to the Matsubara frequency M . The concept of particles being on, close or off their “mass-shell” used throughout this paper to describe screening physics has the precise meaning given by this interpretation of the singularities in p_1 in the original four-dimensional static correlators. It should be emphasized that the screening singularities we have introduced here have no direct relation to real-time dynamics, which corresponds to singularities in real frequency in the (3+1)-dimensional nonstatic correlators [2].

Finally, it is helpful to remind here that thermodynamical quantities are determined from static Green’s functions in the kinematic region with vanishing or small external momenta, in contrast with the screening physics directly involving quarks mentioned above.

B. Criteria for dimensional reduction

1. Pure bosonic case

DR in the bosonic sector can be explained by the observation that there exists a clear scale separation when temperature is high enough. Modes with non-vanishing Matsubara frequencies have masses of order T , while modes with zero Matsubara frequency have masses of order one. If one is only interested in the dynamics of the static modes in the low momentum regime, nonstatic modes might play negligible role, since their effects can only be felt through virtual processes with energies comparable to or higher than their masses.

The above intuitive picture can be formalized within the framework of perturbation theory in the following way. The $(D+1)$ -dimensional Lagrangian \mathcal{L}^{D+1} is said to undergo DR to a specific D -dimensional Lagrangian \mathcal{L}^D , in the high- T limit and to a given order in the coupling constant, if all the *static* Greens' functions of \mathcal{L}^{D+1} , $G^{D+1}(\mathbf{p}, T)$, are equal to the corresponding Green's functions of \mathcal{L}^D , $G^D(\mathbf{p})$, up to corrections suppressed by powers of $1/T$:

$$G^{D+1}(\mathbf{p}, m, T) = G^D(\mathbf{p}, m) + \mathcal{O}(|\mathbf{p}|/T, m/T), \quad (1)$$

where m represents possible external dimensionful parameters of the theory, such as a usual mass parameter. In general, the form and the parameters of \mathcal{L}^D are determined by the original theory.

These naive expectations based on a tree-level power counting fail because of dynamically generated scales of order T [11]. Nevertheless, these dynamically generated scales only induce corrections proportional to powers of the coupling. If the coupling is small, the concept is still useful and the reduced theory still provides a simplified physics picture.

It is apparent that if the original theory is renormalizable in $D+1$ dimensions, the reduced theory is a super-renormalizable theory in general, since the coupling in the reduced theory will have positive dimension in mass units. However, whether the ultraviolet behavior of the reduced theory is truly improved depends on whether all Matsubara modes, except a finite number, decouple. Finally, we remind that beyond tree-level DR manifests explicitly in the reduced Lagrangian only in certain specific classes of subtraction schemes [8,11], although the physics of DR for a given theory is of course a scheme independent phenomenon. We shall make further comments on this point, when we discuss the choice of the coupling constant in the reduced theory.

2. Fermionic case

Due to the antiperiodic boundary condition in the temporal direction, all fermionic fields have tree-level masses of order T . As a consequence, fermions are usually treated like implicit degrees of freedom in the high- T limit. However, there are situations where we want to study observables that directly involve fermions and that are zero if no explicit fermionic dynamics is kept. A typical example is the correlation between mesonic currents, which is defined in terms of fermionic fields: the Lagrangian does not include terms that couple such currents directly to bosonic fields and the leading contribution is given by fermionic modes. When studying such cases, does it still make sense to ask whether some of the fermionic modes

are more important than others? The naive answer might be negative, since there exists no obvious scale separation between the lightest fermionic modes $\pm\pi T$ and the rest.

This apparent lack of a scale separation is also reflected in the fact that the typical spatial momenta of the fermionic modes at high temperature are not small relative to T . For example, even in the free theory case, fermions are always on their mass-shell and hence $|\mathbf{p}|$ is of the order T . This implies that the expansion in $|\mathbf{p}|/T$ is meaningless.

However, QCD is asymptotically free and quarks are weakly interacting in the high- T limit. As previously discussed, in this weakly interacting regime, quarks are almost on their “mass-shell”. This intuitive picture suggests us that the relevant small scale is not the typical spatial momentum, which is large even in the free theory, but the amount by which the interaction brings the spatial momentum off the free-theory mass-shell (the “off-shellness”) or, in other words, the residual momentum after the contribution from the mass has been subtracted out.

If we consider, for example, one of the lowest Matsubara modes $\omega_{\pm} = \pm\pi T$, we can define the dynamical residual momentum $\mathbf{q}^2 \equiv \mathbf{p}^2 + (\pi T)^2$ and, similarly to the bosonic case, we say that the theory undergoes DR, if all the *static* Greens’ functions $G^{D+1}(\mathbf{p}, T)$ are equal to the corresponding Green’s functions $G^D(\mathbf{p})$ up to corrections suppressed by powers of $1/T$:

$$G^{D+1}(\mathbf{p}, m, T) = G^D(\mathbf{p}, m) + \mathcal{O}(|\mathbf{q}|/T, m/T), \quad (2)$$

where again m represents possible external dimensionful parameters of the theory. Similarly to bosonic cases, corrections are suppressed only by powers of the coupling constants instead of powers of $1/T$ when there are dynamically generated masses proportional to T or, as we shall see, when the specific dynamics makes the residual momentum proportional to T .

3. Analogy with the heavy-quark expansion

The situation we have described for the high- T expansion in the quark sector shows several similarities with the heavy quark expansion in QCD [16–18]. In fact, the heavy quark degrees of freedom can usually be integrated out leaving power suppressed corrections if our interest is in light quark observables, such as the D meson. When we also want to study observables that involve heavy quarks, such as heavy quarkonia, the explicit heavy degrees of freedom must be retained. In addition, the effective theory that describes the heavy quark sector is also derived by expanding in the residual momentum relative to the heavy quark mass.

However, there are two major differences between the heavy quark expansion and the high- T expansion for quarks. One difference is that, in the latter case, we need to integrate out an infinite number of Matsubara modes for each flavor, whereas in the former only the antiquark degree of freedom is integrated out for each flavor. The other difference is that the coupling constant in the high- T reduced theory is, for pure dimensional reasons, proportional to T , while the coupling constant in the heavy-quark effective (HQE) theory, is independent of (or at worst logarithmically dependent on) the heavy quark mass. The first difference leads to the consequence that the HQE theory maintains the original dimensionality $3+1$ and the high- T effective theory has its dimensionality reduced by one. The second difference implies

that, contrary to the HQE theory, the accuracy of the high- T effective theory is usually worsened from powers of $1/T$ to only powers of the coupling.

C. Relevant kinematic region for fermion DR

Following the strategy described at the beginning of this section, we examine here what are the precise kinematic regions where DR can take place in the fermionic sector for fundamental and composite operators.

From now on we call light modes the static gluon ($\Omega_n = 0$) and the lightest quarks ($\omega_n = \pm\pi T$), while the rest of the modes are denoted as the heavy modes.

1. Fundamental fields

An external light quark close to its mass shell has a momentum of the form $p = (\omega_{\pm}, \mathbf{p})$ with $\mathbf{p}^2 \sim -\pi^2 T^2$. For definiteness, let us consider the “particle” characterized by ω_+ : the same considerations can be trivially repeated for the other light mode ω_- . Here and in the following each quark mode of different Matsubara frequency is regarded as a “flavor” in the three-dimensional theory. Quotes are used to distinguish this use of the word “flavor” from the usual one. Since the on-shell condition is defined in Minkowskian space, we choose p_1 as the “time” component or energy in the reduced world (the original time component p_0 becomes a chirally invariant mass). Then the residual momentum is defined as $q_1 = p_1 - i\omega_+$, $q_2 = p_2$ and $q_3 = p_3$ with $|q_i| \ll T$. The alternative choice of $q_1 = p_1 + i\omega_+$ can be interpreted as the interchanging of particle and antiparticle of the same “flavor”.

Of course, one can also choose $p_1 \sim i\omega_n T$ with $n \neq \pm 1$, i.e. p_1 being close to one of the heavy mass-shell. However, the physically most relevant singularities are those closest to the origin in the complex plane of p_1 , since only these are practically measurable on the lattice. Therefore, we only limit ourselves to the cases of $p_1 \sim i\omega_{\pm}$.

A static gluon close to its mass-shell has a momentum of the form $k = (0, \mathbf{k})$ with $|\mathbf{k}| \ll T$. Therefore, the definition of the high- T expansion as an expansion around the mass-shell of the weakly interacting modes reproduces the usual condition when applied to the bosonic sector (pure Yang-Mills case).

2. Composite operators

The rationale underlying the choice of the relevant kinematic regime when composite operators, such as meson and baryon currents, are present is the same as the one used in the quark and gluon sector: we expect small deviations from the free theory.

For a static mesonic current with momentum $k = (0, \mathbf{k})$, the lowest singularity starts at $\mathbf{k}^2 \sim -(2\pi T)^2$, as one can easily verify considering the free fermion-bubble graph. This singularity corresponds to the lowest particle-antiparticle threshold, where particles and antiparticles are defined as the excitations near the two possible mass-shell conditions: $p_1 = i\omega_+$ and $p_1 = -i\omega_+$. To be consistent with this condition, the momenta of the particle and antiparticle in the composite operator have the form $p = (\omega_+, \mathbf{p})$ and $p' = (\omega_+, \mathbf{p}')$

with $p_1 \sim i\omega_+$ and $p'_1 \sim -i\omega_+$ and $k = p - p'$. The momenta running along the free fermion-bubble show clearly why we call, in the reduced theory, quarks with the same p_0 but “opposite” p_1 components particle and antiparticle, while we distinguish quarks with different p_0 components using different “flavor”.

We could perform a similar analysis for baryonic currents. Since we do not anticipate any further conceptual problem in this kind of extension, we consider in this work only mesonic currents.

D. Expansion parameter and power counting

1. Tree level

In the relevant kinematic region, we can classify propagators according to their behavior close to mass-shell and then construct a corresponding power-counting scheme that characterizes the behavior of a given graph. For example, it is trivial to verify that, when close to mass-shell, a light-fermion propagator is of the order $T/|\mathbf{q}|$, while a static gluon propagator is of the order of T^2/\mathbf{k}^2 , relative to propagators of heavy modes.

The energy-momentum conservation at each vertex forces internal quark lines of a graph whose external lines are close to their mass-shell to remain themselves close to the mass-shell, unless at least one of the internal lines is heavy. However, a graph that involves internal heavy lines is suppressed relative to the same graph with the heavy lines replaced by light ones, as it is trivially demonstrated by the propagator classification given above. This result, in turn, implies that any tree graph with only light external quark or antiquark lines is correctly reproduced by the corresponding tree graph in the reduced theory.

2. Loop effects

The fact that the dominant contributions to screening observables come from the kinematic regions where the external line are close to their mass-shell in the (2+1)-dimensional Minkowskian space implies that the relevant power counting that establishes the relative importance of the difference graphs is not the usual one in Euclidean space. This necessity of explicitly considering the contributions of the Minkowskian singularities makes the power counting for graphs involving loops less straightforward than at the tree level. Fortunately, the number of graphs at a given order in the loop expansion is finite. At the one-loop level this number is small. We can just perform an explicit calculation and isolate the important contributions.

The strategy we adopt is the following. We consider any graph, $G_{4D}(\mathbf{p}, T)$, in the original theory in 3+1 dimensions, where \mathbf{p} is close to the mass-shell, and we then decompose this graph into terms recognizable as three-dimensional graphs. We achieve this result by first separating out those terms in $G_{4D}(\mathbf{p}, T)$ that involve only light lines: these terms are by definition reproduced by the reduced tree-level three-dimensional Lagrangian and we denote them by $G_{3D}(\mathbf{p}, T)$. The remaining contributions to $G_{4D}(\mathbf{p}, T)$ involve at least one heavy line and we define them as $G^H(\mathbf{p}, T)$. We say that DR occurs if all such $G^H(\mathbf{p}, T)$'s can be

made local, i.e. if they result in a polynomial in the residual momentum \mathbf{q} . In other words, DR occurs, if

$$G_{4D}(\mathbf{p}, T) = G_{3D}(\mathbf{p}, T) + G^H(\mathbf{p}, T) = G_{3D}(\mathbf{p}, T) + G^H(0, T) + \mathcal{O}(|\mathbf{q}|/T), \quad (3)$$

where $G^H(0, T)$ has either the form of terms already present in the tree-level reduced Lagrangian (its effect is the renormalization of the relevant parameters) or the form of a new renormalizable vertex. More generally, the reduced theory needs also to contain nonrenormalizable vertices if we want to reproduce graphs to higher orders; these terms can be treated consistently in the context of an effective theory (see Sec. V).

III. THE REDUCED THEORY: CALCULATION

A. The tree-level Lagrangian

At the tree level the reduced theory can be simply obtained by Fourier transforming the QCD Lagrangian and then retaining only the static gluonic fields and the quark fields (after rescaling a factor of \sqrt{T}) with lowest Matsubara frequencies ($\omega_{\pm} = \pm\pi T$),

$$\mathcal{L}_{\text{RD}}^0 = -\frac{1}{4}F_{ij}^a F_{ij}^a - \frac{1}{2}(D_i A_0)^a (D_i A_0)^a + \sum_{l=\pm} \bar{\psi}_l \left[-\left(\omega_l + g_3 A_0^a \frac{\lambda^a}{2}\right) \gamma_0 + i\gamma_i D_i \right] \psi_l, \quad (4)$$

where $F_{ij}^a = \partial_i A_j^a - \partial_j A_i^a - g_3 f^{abc} A_i^b A_j^c$, $(D_i A_0)^a = \partial_i A_0^a - g_3 f^{abc} A_i^b A_0^c$ and $D_i \psi = \partial_i \psi - ig_3 A_i^a (\lambda^a/2) \psi$. For simplicity we have assumed that quarks are massless and have N_f flavors. Figure 1 shows the two vertices of $\mathcal{L}_{\text{RD}}^0$ that involve quarks: the graphical notation is such that a thick (thin) solid line represents a quark with frequency ω_+ (ω_-) and a wiggly line represents a static gluon.

The coupling g_3 is related to the four-dimensional coupling through $g_3^2 = g^2(\mu)T$. At the tree level the subtraction scale μ is not yet specified. Since $\mathcal{L}_{\text{RD}}^0$ is a super-renormalizable theory in three dimensions, all the dynamical scales must be set by the coupling constant $g_3^2 = g^2(\mu)T$ and temperature T .

Of course, once loop corrections are included, the reduced theory in Eq. (4) acquires new vertices and the coupling constant g_3^2 has a more complicated dependence on the original coupling $g^2(\mu)$. For example, g_3^2 can receive corrections such as $g^4(\mu)T$ and so on. However, since QCD is asymptotically free, the appropriately defined coupling constant (DR is only manifest in subtraction schemes that require $\mu \sim T$ [11,19,14]) has the asymptotic behavior $g^2(\mu \sim T) \sim 1/\ln T$. Therefore, the corrections to the tree-level form of g_3 should not modify the fact that the two dynamical scales be $g_3^2 \approx g^2(\mu \sim T)T$ and T itself at high temperature. The criterion according to which we choose $\mu \sim T$ is in general to minimize loop corrections to the leading result. We shall discuss the precise choice of the proportionality constant later in the paper.

The vertices that involve light quarks in the reduced theory, the ones shown in Fig. 1, are not the only vertices present in the original theory. There are additional vertices that involve at least one heavy mode; we show them in Fig. 2 with the notation that a double line stands for a heavy quark mode and a spring-like line stands for a nonstatic gluon mode.

These vertices are collectively called $\Delta\mathcal{L}_H$. In the first vertex the fermionic line does not change its “flavor”, since the gluon is static, and we call it “flavor-conserving”. All the other vertices in Fig. 2 involve a nonstatic gluon and, therefore, the fermionic line changes its “flavor”; we call these vertices “flavor-changing”.

Since we are only interested in graphs with light modes in the external lines, energy-momentum conservation implies that these heavy vertices cannot contribute at the tree level. Our job is to verify whether the corrections induced by these heavy vertices at the one-loop order can be accounted for, in the high- T limit, either by readjusting the parameters of $\mathcal{L}_{\text{DR}}^0$ or by adding additional local and renormalizable vertices.

B. One-loop graphs

In the following calculations we use the dimensional regularization for spatial integrals,

$$\int \frac{d^4k}{(2\pi)^4} \rightarrow T \sum_{n=-\infty}^{\infty} \mu^{2\epsilon} \int \frac{d^{3-2\epsilon}\mathbf{k}}{(2\pi)^{3-2\epsilon}} \equiv T \sum_{n=-\infty}^{\infty} \int [d\mathbf{k}], \quad (5)$$

and the $\overline{\text{MS}}$ subtraction scheme. For convenience, we work in the Feynman gauge and use the Euclidean Feynman rules given by Ramond [20].

The subtraction point μ needs to be proportional to T to make the DR manifest [11], then we define the T -dependent coupling constant

$$\tilde{g}^2(T) \equiv g_{\overline{\text{MS}}}^2(\mu) \quad (6)$$

by choosing

$$\mu = \left(4\pi e^{-\gamma_E - c}\right) T. \quad (7)$$

The temperature independent constant c can be read as a convenient way of parameterizing one of the possible subtraction schemes. The specific choice $c = (N/2 - 2N_f \ln 4)/(11N - 2N_f)$ corresponds, for instance, to the scheme that makes DR optimal for the pure-gluon effective action in the background field method [19]. We shall comment later on alternative choices such as the one that makes DR optimal in terms of the quark-gluon vertex function. In the following we also use the auxiliary coupling

$$\mathcal{G}^2(T) \equiv \tilde{g}^2(T)/(16\pi^2), \quad (8)$$

for the sake of making formulae more compact.

Without any loss of generality, we only show results for cases with external quark-line frequency $\omega = \omega_+ \equiv \pi T$; trivial modifications yield the corresponding results for the other light “flavor” with $\omega = \omega_- \equiv -\pi T$. Moreover, we select the particle sector, which we have defined as the kinematic region where the first component of the spatial momentum is close to $i\omega_+$; again there are only trivial differences for the antiparticle sector, which is defined by the alternative choice of the spatial component being close to $-i\omega_+$, and that is separated from the particle sector by a off-(mass)shellness $2\pi T$.

In the Matsubara-frequency loop-sum, the term with zero frequency can be easily recognized as the contribution from the three-dimensional tree-level Lagrangian itself, up to trivial factors of T . Therefore, when computing the loop corrections due to the heavy Matsubara modes, we leave out the term with $n = 0$, which is the direct contribution from the light modes and it is already generated by the reduced theory.

The calculation of the one-loop amplitudes and their high temperature expansion around the appropriate kinematic regions can be done following a standard procedure, which, in general, involves the following steps:

- (1) combine the denominators by means of the Feynman parameter representation and perform the spatial momentum integral;
 - (2) shift the external momenta: $\mathbf{p} = \mathbf{q} + i\omega_+ \hat{e}_1$ and $\mathbf{p}' = \mathbf{q}' + i\omega_+ \hat{e}_1$;
 - (3) expand the result in terms of the residual momenta over T , e.g. $|\mathbf{q}|/T$;
 - (4) perform the integrals over the Feynman parameters;
 - (5) perform the Matsubara sum and express the result in terms of the Riemann zeta function.
- In the following we only give the final results obtained by the application of the above-described procedure.

1. Quark self-energy

The quark self-energy correction due to heavy modes is found by calculating the graphs drawn in Figs. 3 (b) and (c) with external momentum $p = (\omega_+, \mathbf{p}) = (\omega_+, i\omega_+ + q_1, q_2, q_3)$. The result is:

$$i\Sigma(p) = -C_f \mathcal{G}^2(T) \left\{ \left[(X + 2c) p \cdot \gamma + X_{\mu\nu} p_\mu \gamma_\nu \right] + \mathcal{O}\left(\frac{|\mathbf{q}|}{T}\right) \right\}, \quad (9)$$

where $C_f = (N^2 - 1)/(2N)$ and the coefficients X and $X_{\mu\nu}$ are pure numbers that are listed in Table I. In this Table there appear the derivative of the Riemann zeta function evaluated at -1 , $\zeta'(-1)$, and the Euler's constant gamma γ_E , whose approximate numerical values are $\zeta'(-1) \approx -0.16542$ and $\gamma_E \approx 0.57722$.

We find that the heavy mode correction to the self-energy $\Sigma(p)$ is suppressed relative to the tree-level piece $ip \cdot \gamma$ by the factor $\mathcal{G}^2(T)$. In addition, we also point out that, as expected, no chiral-symmetry-breaking mass-term for the quark self-energy has been perturbatively generated, in spite of the fact that other noncovariant terms have instead appeared.

2. Quark-gluon vertex

The corrections of the heavy modes to the quark-gluon vertex come from two types of graphs: graphs that have an analogue in QED, Figs. 4 (b) and (c), and graphs that are intrinsically nonabelian, Figs. 4 (e) and (f). In the following the momentum of the incoming quark is labeled by $p = (\omega_+, \mathbf{p}) = (\omega_+, i\omega_+ + q_1, q_2, q_3)$ and the momentum of the outgoing quark by $p' = (\omega_+, \mathbf{p}') = (\omega_+, i\omega_+ + q'_1, q'_2, q'_3)$.

The first type of graphs yields:

$$\Gamma_\mu(p, p') = i\tilde{g}(T)\frac{\lambda^a}{2}\left(C_f - \frac{C_{ad}}{2}\right)\mathcal{G}^2(T)\left\{[(Y + 2c)\gamma_\mu + Y_{\mu\nu}\gamma_\nu] + \mathcal{O}\left(\frac{|\mathbf{q}|}{T}, \frac{|\mathbf{q}'|}{T}\right)\right\}, \quad (10)$$

where $C_{ad} = N$ and the coefficients Y and $Y_{\mu\nu}$ are given in Table I.

The second type of graphs yields:

$$\Gamma'_\mu(p, p') = i\tilde{g}(T)\frac{\lambda^a}{2}C_{ad}\mathcal{G}^2(T)\left\{[(Z + 3c)\gamma_\mu + Z_{\mu\nu}\gamma_\nu] + \mathcal{O}\left(\frac{|\mathbf{q}|}{T}, \frac{|\mathbf{q}'|}{T}\right)\right\}, \quad (11)$$

and again the coefficients Z and $Z_{\mu\nu}$ are listed in Table I.

In Table I one can notice that there exist precise relations between some of the entries for the quark self-energy (X 's) and of the abelian part of the quark-gluon vertex (Y 's): the reason of these relations is the existence of generalized QED-like Ward identities at finite temperature, due to the static gauge invariance. The fact that our results verify these Ward identities serves as a very useful consistency check.

We find again that the heavy mode corrections to the tree-level coupling coming from $\Gamma_\mu(p, p')$ and $\Gamma'_\mu(p, p')$ are suppressed relative to the tree-level piece $-i\tilde{g}(T)\gamma_\mu$ by the factor $\mathcal{G}^2(T)$. In addition, there are also new vertices not present at $T = 0$, but these vertices are also order of $\mathcal{G}^2(T)$ relative to $-i\tilde{g}(T)\gamma_\mu$.

3. Vacuum polarization

The contributions to the vacuum polarization tensor coming from both light and heavy quarks are given by the graphs shown in Figs. 5 (a), (b) and (c). There are a few small differences relative to the previous two cases. One is that we can consider the three graphs together and we do not need to separate out the contribution from the lowest modes, since all three are infrared finite. In addition, the external gluon line is static $k = (0, \mathbf{k})$ and the loop Matsubara sum is now fermionic $p = (\omega_n, \mathbf{p})$, with $\omega_n = (2n - 1)\pi T$.

In the magnetic sector $\Pi_{ij}(\mathbf{k})$ remains transverse

$$\Pi_{ij}(\mathbf{k}) = (k_i k_j - \mathbf{k}^2 \delta_{ij})\delta_{ab}N_f \frac{g^2(\mu)}{24\pi^2} \left\{ \frac{1}{\epsilon} + \gamma_E + \ln\left(\frac{4\mu^2}{\pi T^2}\right) + \mathcal{O}\left(\frac{\mathbf{k}^2}{T^2}\right) \right\}. \quad (12)$$

After renormalizing at the scale $\mu = 4\pi e^{-\gamma-c}T$, we see that the only effect of Π_{ij} is to give a finite wave-function renormalization to the static gluon compared to the zero temperature case.

We also find that $\Pi_{i0} = \Pi_{0i} = 0$, which in turn implies that there is no mixing between electric and magnetic components in the static sector induced by the nonstatic modes.

The result for the electric part is

$$\Pi_{00}(\mathbf{k}) = -\delta_{ab}N_f \frac{g^2(\mu)}{24\pi^2} \left\{ 4\pi^2 T^2 + \mathbf{k}^2 \left[\frac{1}{\epsilon} + \gamma_E + \ln\left(\frac{4\mu^2}{\pi T^2}\right) - 1 \right] + \mathcal{O}\left(\frac{\mathbf{k}^2}{T^2}\right) \right\}. \quad (13)$$

After the wave-function renormalization, which again only receives a finite contribution with respect to the zero temperature case, we are still left with an additional T^2 term that implies a mass generation for the time component of the static gluon field, which is the well-known analogue of the Debye screening in QED.

C. Summary of one-particle irreducible graphs

The effect of the heavy modes of the original four-dimensional Lagrangian, which are no longer present in the reduced theory, can be reproduced, at the one-loop level and in the relevant kinematic region, by the following three types of corrections to the tree-level (2+1)-dimensional reduced Lagrangian.

- (a) The quark bubble insertion corrects the static gluon propagator and is suppressed by a factor $\mathcal{G}^2(T)$. It also generate a mass term of order $\mathcal{G}^2(T)T^2$ for A_0 .
- (b) The quark self-energy insertion corrects the lightest quark or antiquark propagator and, in addition, generates new terms that are not present at zero temperature. Corrections and new terms are all suppressed by a factor $\mathcal{G}^2(T)$.
- (c) The static gluon-quark vertex insertion corrects the tree-level vertex and generate new vertices. Again corrections and additional vertices are suppressed by a factor $\mathcal{G}^2(T)$.
- (d) In this section we only considered graphs explicitly involving quark fields. Since the on-shell condition for bosonic fields are the same with or without the presence of fermions, graphs containing purely gluons or ghosts have already been considered in Refs. [11,12].

In summary, we find two kinds of corrections in the infrared limit, namely when the light modes are close to their mass-shell. There are corrections that are directly generated by the corresponding one-loop graphs in the reduced theory, once the coupling constant is properly chosen. In addition, there are also one-loop corrections that are not contained in the tree-level reduced theory. However, all these terms are infrared finite to the order considered and are suppressed by a factor $\mathcal{G}^2(T)$ and hence subleading. The fact that this corrections are infrared finite implies that they can be accounted for by adding new local and renormalizable vertices to the reduced theory.

IV. COMPOSITE OPERATORS

In confined theories, such as QCD, the fundamental degrees of freedom are not manifest in the spectrum and it is necessary to use composite operators to probe physical particles of the theory. For example, one uses composite operators as interpolating fields for mesonic and baryonic states. Therefore, the study of how composite operators are reproduced in the reduced theory is necessary to have a complete picture of the DR physics. We shall find that considering composite operators introduces new features that are not trivial extensions of what already discussed.

For the sake of concreteness, we focus our attention on flavor nonsinglet mesonic currents. Generalization to other cases, such as baryonic operators, can be done analogously. At the tree level, the static limit of these currents can be written as a sum over Matsubara modes

$$\mathcal{O}_\Gamma \equiv \int d\tau \bar{\psi}(\tau, \mathbf{x}) \Gamma \psi(\tau, \mathbf{x}) \propto \sum_n \bar{\psi}_n(\mathbf{x}) \Gamma \psi_n(\mathbf{x}), \quad (14)$$

where Γ is any of the sixteen Dirac matrices. As discussed in Sec. II, the kinematic region of interest is the one where the lightest modes are close to their mass-shell: $2\pi T$ in mesonic and $3\pi T$ in baryonic cases, respectively. Then at the tree level the high temperature limit implies that the dominant contribution comes from the operator obtained by using only the lowest Matsubara quark modes.

A. One-loop correction

The procedure for calculating the one-loop correction to composite operators is similar to the one used for calculating the one-loop vertex correction, except that the momentum carried by the composite operator is now close to the particle-antiparticle mass-shell, in contrast with the momentum carried by a static gluon in the vertex correction. The explicit graphs are shown in Figs. 6 (a), (b) and (c). The choice of the flavor nonsinglet current avoids the mixing with gluonic fields¹.

More specifically, the external quark and antiquark momenta are expanded according to $\mathbf{p} = \mathbf{q} + i\omega_+ \hat{e}_1$ and $\mathbf{p}' = \mathbf{q}' - i\omega_+ \hat{e}_1$, where \mathbf{q} and \mathbf{q}' are supposed to be small relative to T . This choice reproduces the expected on-shell condition for mesonic currents $\mathbf{p} - \mathbf{p}' \approx 2i\omega_+ \hat{e}_1$. Since this kinematic difference implies a new feature, we give more details in this case.

The one-loop correction to the composite operator is proportional to

$$\Delta\mathcal{O}_\Gamma = g^2(\mu) C_f V_{\mu\nu}(p, p') \gamma_\alpha \gamma_\mu \Gamma \gamma_\nu \gamma_\alpha, \quad (15)$$

where $V_{\mu\nu}(p, p')$ is defined as

$$V_{\mu\nu}(p, p') \equiv 2T \sum_{n \neq 0} \int [d\mathbf{k}] \int_0^1 d\alpha \int_0^{1-\alpha} d\beta \frac{(p+k)_\mu (p'+k)_\nu}{\left[(1-\alpha-\beta)k^2 + \alpha(p+k)^2 + \beta(p'+k)^2 \right]^3}. \quad (16)$$

This definition obviously implies that $V_{\mu\nu}(p, p') = V_{\nu\mu}(p', p)$. The term in the Matsubara sum with $n = 0$, which is represented in Fig. 6 (a), has been excluded from $V_{\mu\nu}$, since this term is directly reproduced by the reduced theory $\mathcal{L}_{\text{RD}}^0$, given by Eq. (4).

Fig. 6 (c), i.e. the terms with $n \neq -1, 0$, can be checked to be infrared finite; their explicit contribution to $V_{\mu\nu}(p, p')$ is, up to corrections of $\mathcal{O}(|\mathbf{q}|/T, |\mathbf{q}'|/T)$,

$$V_{00}^{(c)}(p, p') = \frac{1}{64\pi^2} \left\{ \frac{1}{\epsilon} + \ln\left(\frac{\mu^2}{4\pi T^2}\right) + \gamma_E + W_{00} \right\}, \quad (17a)$$

$$V_{ij}^{(c)}(p, p') = \frac{\delta_{ij}}{64\pi^2} \left\{ \frac{1}{\epsilon} + \ln\left(\frac{\mu^2}{4\pi T^2}\right) - \gamma_E \right\} + \frac{\delta_{i1}\delta_{j1}}{64\pi^2} W_{11}, \quad (17b)$$

$$V_{01}^{(c)}(p, p') = -V_{10}^{(c)}(p, p') = -\frac{i}{64\pi^2} W_{01}, \quad (17c)$$

$$V_{0i}^{(c)}(p, p') = -V_{i0}^{(c)}(p, p') = 0 \quad \text{for } i = 2, 3, \quad (17d)$$

where the numerical coefficients W_{00} , W_{11} , and W_{01} are given in Table I. After taking care of the $1/\epsilon$ terms, which have exactly the same form as at $T = 0$, using the standard composite operator renormalization, there only remain the infrared finite terms that can be reproduced by correcting the tree-level current \mathcal{O}_Γ in the reduced theory with the addition of local operators.

¹States that mix with gluonic fields are dominated by the bosonic zero modes and can be described by the pure glue reduced theory with the addition of local operators that couple quarks and gluonic states.

B. Additional infrared singularity

Now let us focus on the remaining term shown in Fig. 6 (b), corresponding to $n = -1$ in $V_{\mu\nu}(p, p')$ of Eq. (16). In this term a heavy gluon of frequency $\Omega_n = -2\pi T$ is exchanged with a corresponding change of the “flavor” (frequency) of the quarks at the vertices. The expansion around the mass-shell of this term yields, apart from terms of $\mathcal{O}(|\mathbf{q}|/T, |\mathbf{q}'|/T)$,

$$V_{\mu\nu}^{(b)}(p, p') = \frac{1}{16\pi^2} \times \int_0^1 d\alpha \int_0^{1-\alpha} d\beta \frac{\delta_{\mu 0} \delta_{\nu 0} + i\delta_{\mu 0} \delta_{\nu 1}(1 - \alpha + \beta) - i\delta_{\mu 1} \delta_{\nu 0}(1 + \alpha - \beta) + \delta_{\mu 1} \delta_{\nu 1}[1 - (\alpha - \beta)^2]}{[(2 - \alpha - \beta)^2 + 2a\alpha(1 - \alpha) + 2b\beta(1 - \beta) - 2\alpha\beta(2 - a - b)]^{3/2}}, \quad (18)$$

where $a \equiv iq_1/(\pi T)$ and $b = -iq'_1/(\pi T)$. The Feynman-parameter integrals can be carried out with the result

$$V_{\mu\nu}^{(b)}(p, p') = -\frac{\ln(a+b)}{64\pi^2} [\delta_{\mu 0} \delta_{\nu 0} + i\delta_{\mu 0} \delta_{\nu 1} - i\delta_{\mu 1} \delta_{\nu 0} + \delta_{\mu 1} \delta_{\nu 1}] + \frac{1}{32\pi^2} [\delta_{ij} + \delta_{i1} \delta_{j1}(4 \ln 2 - 3)] + \mathcal{O}\left(\frac{|\mathbf{q}|}{T}, \frac{|\mathbf{q}'|}{T}\right), \quad (19)$$

which is clearly logarithmically divergent in the infrared.

The situation is summarized as follows.

- (1) The term represented by the graph in Fig. 6 (a) diverges linearly and gives the leading infrared contribution coming from the composite operator: this term only involves the lowest Matsubara modes and, therefore, its infrared physics is exactly reproduced by the reduced theory $\mathcal{L}_{\text{DR}}^0$.
- (2) The terms represented by the graph in Fig. 6 (c) are infrared finite: these terms involve heavy Matsubara modes and their contribution is not generated by the tree-level reduced Lagrangian $\mathcal{L}_{\text{RD}}^0$, but they can be compensated by adding new local operators to \mathcal{O}_Γ .
- (3) The term represented by the graph in Fig. 6 (b) diverges logarithmically and gives a subleading infrared contribution compared to graph (a): this term involves the lowest Matsubara modes for the quark lines and a heavy mode for the gluon line and, therefore, it is not present in the reduced theory. In addition, this infrared logarithmic behavior apparently implies that it cannot be generated by adding a local correction to the operator. In other words, we need to settle the question whether it is possible to add to the tree-level operator in the reduced theory higher-dimensional operators that might generate the same logarithmic singularity. This option is easily ruled out, once one recognizes that this logarithmic singularity is associated with the total external momentum carried by the composite current $q_1 - q'_1$ and is related to the particle-antiparticle (of the “-” mode) production threshold, as can be seen explicitly from Fig. 6 (b).

We are left with the option of adding a higher-dimensional vertex to the reduced theory. We can easily guess the form of this new vertex from the fact that the logarithmic singularity comes from the kinematic region of Fig. 6 (b) where the particle and antiparticle are close to their mass-shell, while the heavy gluon is far off its mass-shell, i.e. the gluon line “contracts” to a point. In fact, integrating out the heavy gluon yields the four-quark vertex

$$\Delta\mathcal{L}_F = \frac{\tilde{g}^2(T)}{4\pi^2 T} \left(\bar{\psi}_+ \gamma_\mu \frac{\lambda^a}{2} \psi_- \right) \left(\bar{\psi}_- \gamma_\mu \frac{\lambda^a}{2} \psi_+ \right), \quad (20)$$

which is depicted in Fig. 7 (a). If we add this four-quark vertex to the reduced Lagrangian, there appears a new contribution, shown in Fig. 7 (b), to the composite operator one-loop calculation. This new contribution gives the same logarithmic singularity of Eq. (19)

$$\begin{aligned} \Delta V_{\mu\nu}(p, p') &= -\frac{\ln(a+b)}{64\pi^2} [\delta_{\mu 0}\delta_{\nu 0} + i\delta_{\mu 0}\delta_{\nu 1} - i\delta_{\mu 1}\delta_{\nu 0} + \delta_{\mu 1}\delta_{\nu 1}] \\ &+ \frac{1}{32\pi^2} [(\delta_{\mu 0}\delta_{\nu 0} + i\delta_{\mu 0}\delta_{\nu 1} - i\delta_{\mu 1}\delta_{\nu 0} + \delta_{\mu 1}\delta_{\nu 1}) \ln 2 - (\delta_{i1}\delta_{j1} + \delta_{ij})/2], \end{aligned} \quad (21)$$

while the finite differences can now be compensated by local corrections to the operator.

Of course, if we add this new four-quark vertex to the reduced Lagrangian, we need also to consider its additional contribution to the fundamental one-particle irreducible graphs which have already been calculated in Sec. III. In particular, we must check that the corrections to those graphs induced by this four-quark term are infrared finite. At the one-loop level, we need to consider only two graphs: the one depicted in Fig. 7 (c), which contributes to the fundamental vertex, and the one depicted in Fig. 7 (d), which contributes to the quark self-energy. An explicit calculation shows that these two contributions are indeed infrared finite. Explicitly, the correction to the vertex, Fig. 7 (c), is

$$\tilde{\Gamma}_\mu(p, p') = -i\tilde{g}(T) \frac{\lambda^a}{2} \left(C_f - \frac{C_{ad}}{2} \right) \mathcal{G}^2(T) \left\{ \gamma_0 \gamma_\mu \gamma_0 + \mathcal{O}\left(\frac{|\mathbf{q}|}{T}, \frac{|\mathbf{q}'|}{T}\right) \right\}, \quad (22)$$

while the correction to the self-energy, Fig. 7 (d), contributes to the chirally invariant mass:

$$i\tilde{\Sigma}(p) = C_f \mathcal{G}^2(T) [2\omega_+ \gamma_0]. \quad (23)$$

Finally, one might worry that the four-quark term given in Eq. (20), since its mass dimension is four, might be nonrenormalizable in the reduced theory, at least by a naive power-counting argument. However, the use of dimensional regularization makes all graphs shown in Figs. 7 ultraviolet finite. In fact, it is the very fact that this operator has mass dimension four that makes its contribution, which is suppressed by one power of $1/T$ at the tree level ($\Delta\mathcal{L}_F \sim 1/T$), be actually only suppressed by $\tilde{g}^2(T)$ in the one-loop graphs of Figs. 7 (b), (c) and (d).

C. Comments to the one-loop calculation

In principle, one could go on and examine higher orders in the loop expansion. However, this additional effort is useless in this framework. In fact, the naive expansion in powers of $1/T$ is only possible, in general, to the leading order in $\tilde{g}^2(T)$. First, thermal masses are eventually generated at some order in the coupling and these masses break the implicit assumption that all the relevant momenta can be made small at will. Second, the power counting argument that is discussed in the next section shows that the residual momenta (off-shellness) in quantities such as screening masses is of the order $q^2 \sim \tilde{g}^2(T)T^2$, which implies that terms proportional to q^2/T^2 are not suppressed by power of $1/T$ but only by powers of $\tilde{g}^2(T)$, which vanishes only logarithmically.

At this point we could write down the reduced theory at the one-loop level, utilizing the calculations done earlier in the last and this sections. However, one important point about the expansion of the off-shellness is the following. When we choose the first component of the momentum (p_1) to be close to either $\pm i\pi T$ as the starting point of the off mass-shell expansion, this choice breaks the symmetry between what we call particle and antiparticle in the reduced theory. If we insist that the reduced theory be formally relativistic, this asymmetry results in the entanglement of corrections of different orders in $\tilde{g}^2(T)$ at a given order in loop expansion. In other words, the heavy quarks of the (2+1)-dimensional reduced theory become nonrelativistic (NR) in the high- T limit, as we shall see in the next section, and the relativistic formalism has the effect of retaining degrees of freedom that are higher order than the ones already dropped. Therefore, the achievement of an accuracy better than the leading order requires the systematic separation of the particle and antiparticle contributions, together with the correct counting of the contributions from the “flavor-changing” term of Eq. (20). We then postpone the explicit expression of the reduced Lagrangian to the next section, where we discuss this more systematic nonrelativistic reduction.

V. NONRELATIVISTIC EFFECTIVE THEORY

The possibility of describing the high- T QCD screening physics by a renormalizable local Lagrangian in 2+1 dimension, is valid only up to one-loop level. However, since our specific goal is to study the screening physics, it still makes sense to give up the renormalizability and derive an effective action for solving screening states in the high- T limit with accuracy better than the leading order. In fact, the effective action necessarily contains higher dimensional operators. The coefficients of these higher dimensional operators will be derived by using the so-called matching technique, in close analogy with the nonrelativistic reduction applied to the positronium [16] in QED and to heavy-quark systems [17] in QCD.

In this section we derive a (2+1)-dimensional effective theory that describes screening states with accuracy up to $\tilde{g}^4(T)$, apart from an overall additive zero-point energy which we determine only up to $\tilde{g}^2(T)$. As discussed at the end of the previous section, this expansion requires an explicit separation of the particle and antiparticle sectors, because of the asymmetry of the mass-shell condition. Therefore, this new theory, which improves results for screening mass splittings by one order in $\tilde{g}^2(T)$, becomes necessarily nonrelativistic-like for quarks.

The basic strategy is the following. We write down the most general nonrelativistic Lagrangian, with terms up to some power in the appropriate power counting scheme. Then the coefficients of these terms are chosen so that they reproduce Green’s functions of the original theory expanded up to the same power in the coupling in the relevant kinematic region.

A. Notations

Since we are interested in the regime of the reduced theory where quarks are close to their mass-shell, in the sense discussed in Sec. II, it is convenient to explicitly rotate from an Euclidean notation (lower case letters) to a Minkowskian notation (upper case letters).

We rotate the original first spatial direction to the time direction of the (2+1)-dimensional theory, while the other two spatial directions remain the spatial directions of the (2+1)-dimensional theory: from now on, bold face letters indicate these two-dimensional vectors. We label the original time direction as the third axis, which now represents the chirally invariant mass in the reduced theory. Specifically, the momentum of a quark mode with tree-level mass $M = \pi T$ is rotated according to

$$(p_0 = iM, p_1, p_2, p_3) \rightarrow ((M + P_0) = -ip_1, P_1 = p_2, P_2 = p_3, M = p_0) \equiv ((M + P_0), \mathbf{P}, M).$$

The related rotation of the Dirac matrices is

$$(\gamma_0, \gamma_1, \gamma_2, \gamma_3) \rightarrow (\Gamma_0 = i\gamma_1, \Gamma_1 = -\gamma_2, \Gamma_2 = -\gamma_3, \Gamma_3 = -\gamma_0) \equiv (\Gamma_0, \mathbf{\Gamma}, \Gamma_3).$$

We use for the matrices Γ the explicit form of Itzykson and Zuber [21]: $\Gamma_0 = \sigma_3 \otimes I_{2 \times 2}$, $\mathbf{\Gamma} = i\sigma_2 \otimes \boldsymbol{\sigma}$, and $\Gamma_3 = i\sigma_2 \otimes \sigma_3$. This choice of the Γ matrices yields the following explicit form of the on-shell spinors, which are defined by $[E(\mathbf{P})\Gamma_0 - \mathbf{P} \cdot \mathbf{\Gamma} - M\Gamma_3]U(\mathbf{P}) = 0$ and $[E(\mathbf{P})\Gamma_0 - \mathbf{P} \cdot \mathbf{\Gamma} + M\Gamma_3]V(\mathbf{P}) = 0$,

$$U(\mathbf{P}) = \frac{1}{\sqrt{2}E(\mathbf{P})} \begin{pmatrix} \boldsymbol{\sigma} \cdot \mathbf{P} + \sigma_3 M \\ E(\mathbf{P}) \end{pmatrix}, \quad V(\mathbf{P}) = \frac{1}{\sqrt{2}E(\mathbf{P})} \begin{pmatrix} \sigma_3 E(\mathbf{P}) \\ -\sigma_3 \boldsymbol{\sigma} \cdot \mathbf{P} - M \end{pmatrix}, \quad (24)$$

where $E(\mathbf{P}) = \sqrt{M^2 + \mathbf{P}^2}$ is the on-shell energy of a free quark in the reduced theory. These spinors specify the basis in which the relativistic 4-component quark field is decomposed as the nonrelativistic 2-component (spin up and down) particle field and 2-component antiparticle field.

For convenience, we also rename the original gauge fields in the reduced theory as: $A_1 = \mathcal{A}_0$, $(A_2, A_3) = \mathcal{A}$ and $A_0 = \varphi$. Since in the reduced theory φ transforms like a matter field under the original static gauge transformation, it is often called the ‘‘Higgs’’ field.

B. Dimensional analysis

In general, the expansions in powers of $\tilde{g}^2(T)$ and in derivatives (or low momenta) are two independent expansions. However, when we consider bound states (screening states in our case) that are dominated by the perturbative interaction, the two expansions become intertwined. The reason is that the typical momentum is no longer an independent variable, but rather it is determined by the interaction, in contrast with scattering experiments where one controls the momenta externally. If the interaction is weak, the typical momentum is proportional to some power of $\tilde{g}^2(T)$.

It is possible to develop a systematic method for counting the contribution of each term in powers of the coupling constant to this combined expansion. The rationale of this method is described in detail in Ref. [17], and it is basically based on the analysis of the relevant Schrödinger equation with a potential derived from the tree-level approximation: in our case $V(\mathbf{x}) \sim g^2 T \ln |\mathbf{x}|$. The resulting power-counting rules valid for studying screening states (bound states of the reduced theory in 2+1 dimensions) are shown in Table II.

It is important to emphasize that the power counting is determined by the leading behavior of the potential in terms of the coupling constant. Therefore, it is still valid even

when the potential acquires a nonperturbative linear confining term. In fact, in the high- T limit the perturbative tree-level potential overwhelms the induced spatial string tension $\sigma_s(T) \propto \tilde{g}^4(T)T^2$ [22].

Quarks in the reduced theory are very heavy making the time direction special relative to the spatial ones: this fact is reflected in the form of the effective Lagrangian, which is nonrelativistic, and also in the power counting rules of Table II

C. Tree level

At the tree level there are two kinds of corrections to the tree-level NR Lagrangian: kinematics corrections and corrections to the elastic scattering of a quark from external sources.

We do not need to consider inelastic scattering, because we impose that the reduced theory contain only one power of the time derivative ∂_t : this requirement corresponds to the precise choice of the field parameterization given in the U and V basis. There are no inelastic terms at the tree level in the original theory, and the inelasticity only appears at the one-loop level with this specific choice. In principle, one can relate this particular choice of the field parameterization to others that involve higher power of ∂_t using the invariance of the physics under field redefinition.

According to the power counting rules shown in Table II, the only corrections up to order $\tilde{g}^4(T)$ relative to the leading term are the following ones.

(a) Kinematics correction:

$$\bar{U}(\mathbf{P})P \cdot \Gamma U(\mathbf{P}) = M + P_0 - E(\mathbf{P}) = P_0 - \frac{\mathbf{P}^2}{2M} + \frac{\mathbf{P}^4}{8M^3}. \quad (25)$$

(b) Scattering from external \mathcal{A}_0 :

$$\begin{aligned} & \bar{U}(\mathbf{P})\tilde{\mathcal{A}}_0(\mathbf{P} - \mathbf{P}')\Gamma_0 U(\mathbf{P}') \\ &= \tilde{\mathcal{A}}_0(\mathbf{P} - \mathbf{P}') \left[1 - \frac{1}{4M^2}(\mathbf{P} - \mathbf{P}')^2 + \frac{i}{2M^2}\sigma_3 \mathbf{P} \times \mathbf{P}' + \frac{i}{2M}\boldsymbol{\sigma} \times (\mathbf{P} - \mathbf{P}') \right]. \end{aligned} \quad (26)$$

(c) Scattering from external \mathcal{A} :

$$\bar{U}(\mathbf{P})\tilde{\mathcal{A}}(\mathbf{P} - \mathbf{P}') \cdot \Gamma U(\mathbf{P}') = \tilde{\mathcal{A}}_i(\mathbf{P} - \mathbf{P}') \left[\frac{1}{2M}(P_i + P'_i) - \frac{i}{2M}\epsilon_{ij}(P_j - P'_j)\sigma_3 \right]. \quad (27)$$

(d) Scattering from external φ :

$$\bar{U}(\mathbf{P})\tilde{\varphi}(\mathbf{P} - \mathbf{P}')\Gamma_3 U(\mathbf{P}') = \tilde{\varphi}(\mathbf{P} - \mathbf{P}') \left[1 - \frac{1}{4M^2}(\mathbf{P}^2 + \mathbf{P}'^2) + \frac{i}{2M}\boldsymbol{\sigma} \times (\mathbf{P} - \mathbf{P}') \right]. \quad (28)$$

D. One-loop level

In Sec. III we have already calculated the heavy mode contributions at one loop. Since now we are using a NR formulation of the reduced theory in the quark sector, the light

quark contributions of the original theory are not exactly equal to the ones in the NR reduced theory, even if they have the same infrared behavior. Therefore, we also need to calculate the one-loop contribution of the light quark modes both in the original theory and in the NR reduced one: the difference between the two results need to be added as a correction to the reduced Lagrangian together with the heavy mode contributions. In addition, the one-loop amplitudes needs to be sandwiched with the appropriate spinors to yield the correct correction terms. The calculation is straightforward and we only list the resulting terms up to $\tilde{g}^4(T)$.

The nonrelativistic one-loop corrections, which need to be compared to the analogous corrections of the light quarks in the original theory, are calculated using the following tree-level Lagrangian

$$\mathcal{L}_{tree}^{NR} = \psi^\dagger \left[iD_t + \frac{\mathbf{D}^2}{2M} - g_3\varphi \right] \psi, \quad (29)$$

where $D_t \equiv \partial_t + ig_3\mathcal{A}_0$, $\mathbf{D} \equiv \boldsymbol{\partial} - ig_3\mathcal{A}$ and ψ now is a two-component (representing spin up and down) nonrelativistic quark field. One can easily work out the Feynman rules associated with this Lagrangian and calculate the relevant one-loop graphs. Again, we only list final results, which have been computed using dimensional regularization.

In the following the one-loop corrections to the original theory both from heavy and light quarks are grouped together (the ones coming from sandwiching with appropriate spinors, the terms calculated in Sec. III and the “new” ones coming from the lowest Matsubara frequency). The one-loop contributions from the NR reduced theory are instead given separately. The explicit values of the X 's, Y 's and Z 's are given in Table II.

(e) Self-energy corrections:

$$\begin{aligned} \bar{U}(\mathbf{P})i\Sigma U(\mathbf{P}) = C_f \mathcal{G}^2(T) & \left\{ -4(M - P_0) \right. \\ & \left. + \left[2M - (X + X_{11} - iX_{10} + 2c)P_0 + (X - X_{00} - iX_{10} + 2c)\frac{\mathbf{P}^2}{2M} \right] \right\}. \end{aligned} \quad (30)$$

$$i\Sigma^{NR} = C_f \mathcal{G}^2(T) \left\{ -2M \left[\frac{1}{\epsilon} - \gamma_E + \ln \frac{\pi\mu^2}{M^2} \right] - P_0 + \frac{3\mathbf{P}^2}{4M} \right\}. \quad (31)$$

The momentum independent divergence in $i\Sigma^{NR}$ is related to the additive mass renormalization in the nonrelativistic Lagrangian. This additive mass term is often explicitly ignored at the price of introducing a zero-point energy ambiguity in the nonrelativistic theory, i.e. we can only calculate mass differences. In principle this ambiguity can be resolved at least perturbatively in each specific regularization scheme.

(f) Abelian-like vertex corrections:

$$\bar{U}(\mathbf{0})\Delta\Gamma_0 U(\mathbf{0}) = i\tilde{g}(T)\frac{\lambda^a}{2}\left(C_f - \frac{C_{ad}}{2}\right)\mathcal{G}^2(T)\left\{-4 + [Y + Y_{11} - iY_{10} + 2c]\right\}. \quad (32)$$

$$\bar{U}(\mathbf{0})\Delta\Gamma_3 U(\mathbf{0}) = i\tilde{g}(T)\frac{\lambda^a}{2}\left(C_f - \frac{C_{ad}}{2}\right)\mathcal{G}^2(T)\left\{-4 + [Y + Y_{00} + iY_{01} + 2c]\right\}. \quad (33)$$

$$\Delta\Gamma_0^{NR} = \Delta\Gamma_3^{NR} = -i\tilde{g}(T)\frac{\lambda^a}{2}\left(C_f - \frac{C_{ad}}{2}\right)2\mathcal{G}^2(T). \quad (34)$$

(g) Nonabelian-like vertex corrections:

$$\bar{U}(\mathbf{0})\Delta\Gamma_0 U(\mathbf{0}) = i\tilde{g}(T)\frac{\lambda^a}{2}C_{ad}\mathcal{G}^2(T)\left\{-2 + [Z + Z_{11} - iZ_{10} + 3c]\right\}. \quad (35)$$

$$\bar{U}(\mathbf{0})\Delta\Gamma_3 U(\mathbf{0}) = i\tilde{g}(T)\frac{\lambda^a}{2}C_{ad}\mathcal{G}^2(T)[Z + Z_{00} + iZ_{01} + 3c]. \quad (36)$$

$$\Delta\Gamma_0^{NR} = \Delta\Gamma_3^{NR} = 0. \quad (37)$$

Since the leading terms are already order $\tilde{g}^3(T)$, the momentum dependent terms are higher orders and can be dropped in vertex corrections.

As expected, the one-loop corrections in the original theory and the NR reduced theory do not match exactly. The differences can be compensated up to order $\tilde{g}^4(T)$ by adding the following terms to the (2+1)-dimensional NR Lagrangian

$$\Delta\mathcal{L}_{1-loop} = \mathcal{G}^2(T)\left\{c_1\psi^\dagger i\partial_t\psi + c_2\psi^\dagger\frac{\partial^2}{2M}\psi - c_3\psi^\dagger g_3\mathcal{A}_0\psi - c_4\psi^\dagger g_3\varphi\psi\right\}. \quad (38)$$

The coefficients c_i 's, which are determined by subtracting the one-loop corrections obtained in the NR reduced theory from those computed in the original theory, are given in Table III.

It is important to realize that we have taken out a factor of 2 from the one-loop results computed in the original theory before we subtract the nonrelativistic results from them. The necessity of dividing out this factor of 2 comes from the fact that the Lagrangian in Eq. (4) has two degenerate ‘‘flavors’’ (with $M = \pm\pi T$), whereas the NR one-loop results are for a single ‘‘flavor’’. If the physics requires a normal flavor structure, the relevant flavor content must be added explicitly to the NR Lagrangian.

E. Reduced Lagrangian: fermionic part

We can now write down the final result for the fermionic part of the DR Lagrangian by collecting the corrections from the last two subsections and properly gauging each derivative.

The final form of this Lagrangian is more suggestive if written in terms of the appropriate color electric and magnetic fields ($i = 1, 2$)

$$\mathcal{E}_i \equiv \mathcal{F}_{0i}, \quad \mathcal{B}_3 \equiv \frac{1}{2}\epsilon_{ij3}\mathcal{F}_{ij}, \quad (39)$$

where $\mathcal{F}_{ij} = \partial_i\mathcal{A}_j - \partial_j\mathcal{A}_i - ig_3[\mathcal{A}_i, \mathcal{A}_j]$ is the gauge field strength tensor in 2+1 dimensions. Note that there is only one component of the color magnetic field in 2+1 dimensions. The final Lagrangian is given by

$$\mathcal{L}_F = \mathcal{L}^{(0)} + \mathcal{L}^{(1s)} + \mathcal{L}^{(2)} + \mathcal{L}^{(2s)}, \quad (40)$$

with

$$\mathcal{L}^{(0)} = \Psi^\dagger\left(iD_t + \frac{\mathbf{D}^2}{2M}\right)\Psi - g_\varphi\Psi^\dagger\varphi\Psi, \quad (41a)$$

$$\mathcal{L}^{(1s)} = -\frac{g_3}{2M}\Psi^\dagger\boldsymbol{\sigma} \times \boldsymbol{\mathcal{E}}\Psi + \frac{g_\varphi}{2M}\Psi^\dagger\boldsymbol{\sigma} \times (\mathbf{D}\varphi)\Psi \quad (41b)$$

$$\mathcal{L}^{(2)} = \frac{g_3}{4M^2} \Psi^\dagger (\mathbf{D} \cdot \boldsymbol{\varepsilon} - \boldsymbol{\varepsilon} \cdot \mathbf{D}) \Psi - \frac{g_\varphi}{4M^2} \Psi^\dagger \{ \mathbf{D}^2, \varphi \} \Psi + \Psi^\dagger \frac{\mathbf{D}^4}{8M^3} \Psi \quad (41c)$$

$$\mathcal{L}^{(2s)} = \frac{g_3}{2M} \Psi^\dagger \sigma_3 \mathcal{B}_3 \Psi + \frac{ig_3}{4M^2} \Psi^\dagger \sigma_3 (\mathbf{D} \times \boldsymbol{\varepsilon} - \boldsymbol{\varepsilon} \times \mathbf{D}) \Psi, \quad (41d)$$

where the sum over the color indices is implicit. In the above equation we have absorbed the one-loop corrections, due to $\Delta\mathcal{L}_{1\text{-loop}}$ in Eq. (38), into finite renormalization of the proper physical quantities:

$$\Psi = \left[1 + \frac{c_1}{2} \mathcal{G}^2(T) \right] \psi, \quad (42a)$$

$$M = \pi T \left[1 + (c_1 - c_2) \mathcal{G}^2(T) \right], \quad (42b)$$

$$g_3 = \tilde{g}(T) \sqrt{T} \left[1 - (c_1 - c_3) \mathcal{G}^2(T) \right], \quad (42c)$$

$$g_\varphi = \tilde{g}(T) \sqrt{T} \left[1 - (c_1 - c_4) \mathcal{G}^2(T) \right]. \quad (42d)$$

At this point it is appropriate to make some general remarks concerning the fermionic effective Lagrangian.

(1) The Lagrangian in Eqs. (40) and (41) has contribution only from a “single-flavor” particle state. The reduced Lagrangian for the antiparticle state has the same form except that couplings change sign. The four-fermion term in Eq. (20) does not give contribution to order $\tilde{g}^4(T)$ because of the separation of the quark and antiquark sectors.

(2) According to the power counting rule in Table II, $\mathcal{L}^{(0)}$ begins to contribute to the binding energy at order $\tilde{g}^2(T)T$, $\mathcal{L}^{(1s)}$ at order $\tilde{g}^3(T)T$, and $\mathcal{L}^{(2)}$ and $\mathcal{L}^{(2s)}$ at order $\tilde{g}^4(T)T$. While $\mathcal{L}^{(0)}$ and $\mathcal{L}^{(2)}$ are spin independent, $\mathcal{L}^{(1s)}$ and $\mathcal{L}^{(2s)}$ are spin-dependent.

(3) Even though there exist NR four-fermion terms that are order $\tilde{g}^4(T)$ according to a naive application of the power-counting rules of Table II, e.g. $g^2(\Psi^\dagger \Psi \Phi^\dagger \Phi)/M$ (Φ is the antiquark field), these terms can only contribute to the binding energy through higher-loop graphs and, therefore, their contributions are in fact of order higher than $\tilde{g}^4(T)$.

(4) Notice that $\mathcal{L}^{(1s)}$ is absent in 3+1 dimensions since it is not a scalar under spatial rotation, while it is a scalar under a two-dimensional rotation around the 3rd direction.

(5) Since the self-energy in the NR theory is specified up to an additive constant, the Lagrangian in Eq. (40) cannot give the zero-point energy. However, it is still possible to determine perturbatively the zero-point energy shift between the NR Lagrangian and the original one. For instance, the formulae given in Eqs. (30) and (31) give the zero-point energy shift up to order $\tilde{g}^2(T)$. If we want to reach the same accuracy we have obtained for the energy differences (splittings), i.e. $\tilde{g}^4(T)$, also for the zero-point energy shift we need to perform a two-loop calculation of the quark self-energy.

(6) The fact that $\mathcal{G}^2(T)$ is small, as we shall see shortly, means that corrections from heavy modes and, therefore, the coefficients of higher dimensional operators are small and can be calculated perturbatively. It does not mean that the physics governed by the DR Lagrangian, whose coupling constant $\tilde{g}^2(T)T$ is very large at high T , is perturbative. In fact, the infrared behavior of the DR Lagrangian, by construction, remains the same as the original theory.

(7) The coefficients in Eq. (40) has been derived in the $\overline{\text{MS}}$ scheme. If one wants to solve the reduced theory in a different renormalization scheme, e.g. on the lattice, one needs, in

principle, to compute again these coefficients in that specific scheme. In practice, this may not be necessary, since $\mathcal{G}^2(T)$ has turned out to be numerically very small and, hence, the tree-level coefficients, which are scheme independent, dominate. One could have problems only in those scheme that have corrections anomalously large.

(8) The full gauge invariance in the original theory is now reduced to the “static” gauge invariance, which is explicitly kept in the above Lagrangian.

(9) In analogy to universality in the pure bosonic case, a similar universality also holds in the quark sector. After the one-particle irreducible graphs have been matched in the relevant kinematic region and the reduced Lagrangian obtained, any other Green’s function can be computed from this same Lagrangian to within the same accuracy of the matching. For example, we expect that the reduced theory is capable of describing the screening states, e.g. those states that describe the spatial correlation of mesonic currents; these states can be interpreted as bound states in the reduced world and hence they are beyond those 1PI graphs we have used to derive the reduced theory. We have explicitly verified this fact in the Gross-Neveu model [14]. In particular, the screening mass splittings can be solved from the reduced theory to an accuracy of $\tilde{g}^4(T)$, though only nonperturbatively.

F. Reduced Lagrangian: bosonic part

For the purpose of describing mesonic and baryonic screening states to order $\tilde{g}^4(T)$, we only need the bosonic part of the Lagrangian \mathcal{L}_B to order $\tilde{g}^2(T)$. In fact, these screening states reduce to two (three) valence quarks in infinite weak coupling (infinite T) limit and, therefore, the gluonic contribution to the binding coming from \mathcal{L}_B has to involve one more loop and hence an additional $\tilde{g}^2(T)$ factor. For this reason, it is sufficient for our purpose to use the bosonic part of the reduced Lagrangian up to one loop, which has already been derived in Refs. [11,12]

$$\mathcal{L}_B = -\frac{1}{4}\mathcal{F}_{\mu\nu}^a\mathcal{F}_{\mu\nu}^a - \frac{1}{2}(D_\mu\varphi)^a(D_\mu\varphi)^a - \frac{1}{2}m_D^2\varphi^a\varphi^a + \dots, \quad (43)$$

where $m_D^2 = \tilde{g}^2(T)(N/3 + N_f/6)T^2$ is the one-loop Debye screening mass, $\mu, \nu = 0, 1, 2$ and the dots represent terms that contribute to the binding energy at orders higher than $\tilde{g}^4(T)$, e.g. the interaction terms between φ and \mathcal{A}_μ .

G. The complete reduced Lagrangian

In summary, the complete reduced theory that should describe mesonic and baryonic screening physics with accuracy up to $\tilde{g}^4(T)$ for mass splittings and up to $\tilde{g}^2(T)$ for the overall mass is given by the sum of quark DR Lagrangian \mathcal{L}_F in Eq. (40), the corresponding antiquark DR Lagrangian, which is still given by Eq. (40) with opposite sign for the couplings, and the gluonic Lagrangian \mathcal{L}_B in Eq. (43). The correspondence between the parameters in QCD and in the reduced theory is given explicitly in Eq. (42), and in Eqs. (6–8). In the kinematic region that is relevant for these screening states, i.e. those states that dominate the large-distance correlation between currents, the lightest quark mode is close

to its mass-shell, and the self-consistency of the reduced theory is guaranteed by the power counting rule given in Table II, which have been justified in Refs. [16,17], exactly in parallel with the heavy quarkonium systems. The essence of the argument is that, if the interaction is weak, the off-shellness is small.

A final word of caution about the usefulness of this reduced theory. Thermodynamic quantities, such as the free energy, specific heat and so on, are dominated by the gluonic zero modes. As it is well-known, quarks are heavy relative to gluonic zero modes and hence their contribution to thermodynamic quantities is suppressed at high T . This is perhaps the reason why quark degrees of freedom have never been considered relevant at high T , until one has been explicitly interested in the mesonic and baryonic screening states. The effective theory we derived is not intended for bulk thermodynamic observables, but only for those screening states that do not mix with purely gluonic states.

H. At what temperature do we expect DR?

At last we have obtained a reduced theory that includes the quark sector and that should be valid in the high- T limit. However, we still face the practical question of estimating the temperature above which this DR theory is going to be a good approximation to QCD.

We know that DR is manifest only in a limited class of subtraction schemes [11], but even within this class there is some freedom left: one aspect of this freedom is the choice of the coupling constant in the reduced theory $g_3^2 \equiv \tilde{g}^2(T)T$. While it is unambiguous how $\tilde{g}^2(T)$ runs with T , the numerical value of $\tilde{g}^2(T)$ at a specific temperature depends on how we match the reduced and the original theory. For instance, we have argued that a physically relevant way of choosing the coupling in the pure gluonic sector is to match the effective actions in the background field scheme [19]. This specific choice yields that DR in the pure glue sector sets in around $2T_c$, i.e. the coupling constant is sufficiently small at that temperature.

This freedom in the choice of the relevant coupling constant can be rephrased in our formalism with the freedom of choosing the scale μ in Eq. (7) where c has different values in different schemes. Since our present interest is to solve screening states of quarks, it might be better to choose the subtraction parameter c with the criterion that the one-loop couplings g_3 and g_φ be as close as possible to their tree-level values. For example, if we demand $c_1 - c_3 = 0$, we get $c = -1/3$ (if $N = 3$). This choice would make the subtraction scale μ defined in Eq. (7) larger than the one obtained from the criterion of optimal DR for gluons, which yields instead $c = 1/22$ ($N = 3$ and $N_f = 0$). Alternatively, if we demand $c_1 - c_4 = 0$, we find a even larger subtraction scale μ ($c = -1.455$).

In either case, the fact that the subtraction scale is larger makes the effective coupling constant at a given temperature smaller in the quark sector than in the pure gluonic sector. This result is certainly in qualitative agreement with the empirical fact that the DR in the quark sector sets in at temperatures almost right above the critical point [6], whereas DR in the pure gluon sector sets in at about $T \approx 2T_c$ [5,22].

VI. SUMMARY AND CONCLUSIONS

We have shown with an explicit one-loop calculation that QCD at high temperature undergoes dimensional reduction also in the quark sector. More specifically, we have shown that static one-particle irreducible graphs contributing to the original four-dimensional correlation functions can be reproduced by a (2+1)-dimensional renormalizable Lagrangian to order $\tilde{g}^2(T)$ in the kinematic region where the lowest Matsubara quark modes are close to their “mass-shell”. Physical reasons why this kinematic region is relevant to screening phenomena have been also discussed. The reduced theory only contains the zero modes of the gauge field and the lowest quark modes as the explicit degrees of freedom and has the form given by Eq. (4) plus the four-fermion term of Eq. (20).

Aiming at a better description of the mesonic and baryonic screening states, we have further improved the reduced theory to order $\tilde{g}^4(T)$ via a nonrelativistic reduction, which results in the reduced effective Lagrangian of Eqs. (40) and (43). In fact, while the relativistic version of the reduced theory mixes different orders in the coupling when used in the kinematic region relevant to screening physics, the nonrelativistic reduction explicitly separates the contribution of particles and antiparticles and allows a correct counting of the expansion parameter.

Furthermore, we have also argued that the reduced theory in the quark sector, i.e. for screening mesonic and baryonic correlators that do not mix with entirely gluonic states, should become accurate at temperatures slightly above the chiral restoration transition temperature, due to the smallness of the appropriate running coupling $\mathcal{G}^2(T)$. In particular, we find that the temperature above which the reduced theory becomes reliable in the quark sector should be even lower than the corresponding temperature in the pure gluonic sector [19]. Our result has the potential for explaining present lattice data [3,4] and provides a formal basis to the recent phenomenological modeling [6] of the same data.

We would like to stress that, although the reduced Lagrangian has been derived in a perturbative context, the reduced theory embodies all the infrared physics of the original theory, i.e. QCD at high temperature. Therefore, the solution of the reduced theory should reproduce the full long-wavelength screening physics of QCD in the high- T limit, which is nonperturbative: nonperturbative approaches such as lattice simulations are required to find this solution. Luckily since the large scale (T) has been explicitly factored out, it is now straightforward to put the nonrelativistic version of the reduced theory on a lattice following, for example, the method of Ref. [17].

ACKNOWLEDGMENTS

One of us (ML) gratefully thanks the Department of Physics at the University of Washington for their hospitality. This work was supported in part by funds provided by the U.S. Department of Energy (DOE) under contract number DE-FG06-88ER40427 and cooperative agreement DE-FC02-94ER40818.

REFERENCES

- * Electronic address: shuang@mitlns.mit.edu
† Present address.
‡ Electronic address: lissia@cagliari.infn.it
- [1] N. P. Landsman and Ch. G. Weert, Phys. Rep. 145 (1987) 141.
 - [2] S. Huang and M. Lissia, Phys. Rev. D 53 (1996) 7270.
 - [3] T. A. DeGrand and C. E. DeTar, Phys. Rev. D 34 (1986) 2469;
C. E. DeTar and J. Kogut, Phys. Rev. Lett. 59 (1987) 399;
S. Gottlieb et al., Phys. Rev. Lett. 59 (1987) 1881;
Y. Koike, M. Fukugita and A. Ukawa, Phys. Lett. B 213 (1988) 497;
K. M. Bitar et al., Phys. Rev. D 43 (1991) 2396;
K. D. Born et al., Phys. Rev. Lett. 67 (1991) 302.
 - [4] C. Bernard et al., Phys. Rev. Lett. 68 (1992) 2125;
S. Schramm and M. -C. Chu, Phys. Rev. D 48 (1993) 2279.
 - [5] A. Irback et al., Nucl. Phys. B 363 (1991) 34;
T. Reisz, Z. Phys. C 53 (1992) 169;
P. Lacey, D. E. Miller and T. Reisz, Nucl. Phys. B 369 (1992) 501.
 - [6] V. Koch, E. V. Shuryak, G. E. Brown and A. D. Jackson, Phys. Rev. D 46 (1992) 3169;
T. H. Hansson and I. Zahed, Nucl. Phys. B 374 (1992) 227;
V. Koch, Phys. Rev. D 49 (1994) 6063;
T. H. Hansson, M. Sporre and I. Zahed, Nucl. Phys. B 427 (1994) 545;
M. Ishii and T. Hatsuda, Phys. Lett. B 338 (1994) 319.
 - [7] P. Ginsparg, Nucl. Phys. B 170 (1980) 388.
 - [8] T. Appelquist and R. D. Pisarski, Phys. Rev. D 23 (1981) 2305.
 - [9] T. Appelquist and J. Carazzone, Phys. Rev. D 11 (1975) 2856.
 - [10] S. Nadkarni, Phys. Rev. D 27 (1983) 917;
A. N. Jourjine, Ann. Phys. 155 (1984) 305;
Alvarez-Estrada, Phys. Rev. D 36 (1987) 2411; Ann. Phys. 174 (1987) 442.
 - [11] N. P. Landsman, Nucl. Phys. B 322 (1989) 498; Comm. Math. Phys. 125 (1989) 643.
 - [12] K. Farakos et al., Nucl. Phys. B 425 (1994) 67;
K. Kajantie et al., Nucl. Phys. B 458 (1996) 90.
 - [13] For a recent review, see E. V. Shuryak, Rev. Mod. Phys. 61 (1993) 1.
 - [14] S. Huang and M. Lissia, Phys. Lett. B 349 (1995) 484.
 - [15] D. J. Gross, R. D. Pisarski and L. G. Jaffe, Rev. Mod. Phys. 53 (1981) 43.
 - [16] W. E. Caswell and G. P. Lepage, Phys. Lett. B 167 (1986) 437.
 - [17] G. P. Lepage et al., Phys. Rev. D 46 (1992) 4052.
 - [18] M. Neubert, Phys. Rep. 245 (1994) 259.
 - [19] S. Huang and M. Lissia, Nucl. Phys. B 438 (1995) 54.
 - [20] P. Ramond, *Field Theory: A Modern Primer* (Addison-Wesley, Reading, MA, 1989).
 - [21] C. Itzykson and J.-B. Zuber, *Quantum Field Theory* (McGraw-Hill, New York, NY, 1980).
 - [22] G. S. Bali et al., Phys. Rev. Lett. 71 (1993) 3059;
F. Karsch et al., Phys. Lett. B 346 (1995) 94.

FIGURES

FIG. 1. Vertices of $\mathcal{L}_{\text{RD}}^0$ that involve only light modes. A wiggly line represents a static gluon, while a thick (thin) solid line represents a quark of frequency ω_+ (ω_-), respectively.

FIG. 2. Vertices of the original Lagrangian that are not present in $\mathcal{L}_{\text{RD}}^0$, since they involve at least one heavy mode ($\Delta\mathcal{L}_{\text{H}}$). A double line denotes a quark of frequency $|\omega_n| \geq 3\pi T$, while a spring-like line denotes a nonstatic gluon mode. The first vertex is “flavor-conserving” and the rest are all “flavor-changing”.

FIG. 3. Feynman graphs for the quark self-energy correction. Graph (a) is generated by $\mathcal{L}_{\text{RD}}^0$, while graphs (b) and (c) involve “flavor-changing” vertices from $\Delta\mathcal{L}_{\text{H}}$. The external quark carries four-momentum $p = (\omega_+, \mathbf{p}) = (\omega_+, i\omega_+ + q_1, q_2, q_3)$.

FIG. 4. Feynman graphs for the quark-gluon vertex correction. Graphs (a) and (d) are generated by $\mathcal{L}_{\text{RD}}^0$, while graphs (b), (c), (e) and (f) involve “flavor-changing” vertices from $\Delta\mathcal{L}_{\text{H}}$. The incoming quark carries four-momentum $p = (\omega_+, \mathbf{p}) = (\omega_+, i\omega_+ + q_1, q_2, q_3)$, and the outgoing antiquark carries four-momentum $p' = (\omega_+, \mathbf{p}') = (\omega_+, i\omega_+ + q'_1, q'_2, q'_3)$, with $|\mathbf{q}| \ll T$ and $|\mathbf{q}'| \ll T$.

FIG. 5. Feynman graphs for the quark contributions to the vacuum polarization tensor. Graphs (a) and (b) are generated by $\mathcal{L}_{\text{RD}}^0$, while graph (c) involves “flavor-conserving” vertices from $\Delta\mathcal{L}_{\text{H}}$. The external gluon carries four-momentum $k = (0, \mathbf{k})$, with $|\mathbf{k}| \ll T$.

FIG. 6. Feynman graphs for the one-loop correction to the composite operator. Graph (a) is generated by $\mathcal{L}_{\text{RD}}^0$, while graphs (b) and (c) involve “flavor-changing” vertices from $\Delta\mathcal{L}_{\text{H}}$. The incoming quark carries the four-momentum $p = (\omega_+, \mathbf{p}) = (\omega_+, i\omega_+ + q_1, q_2, q_3)$, and the outgoing antiquark carries four-momentum $p' = (\omega_+, \mathbf{p}') = (\omega_+, -i\omega_+ + q'_1, q'_2, q'_3)$, with $|\mathbf{q}| \ll T$ and $|\mathbf{q}'| \ll T$.

FIG. 7. Four-quark vertex (a) and its contribution to (b) one-loop correction of composite operators, (c) one-loop correction to the fundamental vertex and (d) one-loop correction to the quark self-energy.

TABLES

TABLE I. One-loop coefficients. The entries that are not listed, i.e. those coefficients with at least one index equal to 2 or 3, are zero.

coefficient	analytic expression	numerical value
X	$2\gamma_E - 24\zeta'(-1) - (14/3)\ln 2 - 1$	0.8898
X_{00}	$X + 1$	1.8898
X_{01}	$i[2\gamma_E - 72\zeta'(-1) - 10\ln 2 - 6]$	$i 0.1332$
X_{10}	$i[X - 1]$	$-i 0.1102$
X_{11}	$i X_{01}$	-0.1332
Y	X	0.8898
Y_{00}	$2\gamma_E + 24\zeta'(-1) + (2/3)\ln 2 + 4$	1.6465
Y_{01}	X_{10}	$-i 0.1102$
Y_{10}	X_{10}	$-i 0.1102$
Y_{11}	X_{11}	-0.1332
Z	$-2\gamma_E + 12\zeta'(-1) + (10/3)\ln 2 + 1/2$	-0.3290
Z_{00}	$\gamma_E - 12\zeta'(-1) - (7/3)\ln 2$	0.9449
Z_{01}	$i[12\zeta'(-1) + (4/3)\ln 2 + 1]$	$-i 0.0609$
Z_{10}	Z_{01}	$-i 0.0609$
Z_{11}	$\gamma_E - 36\zeta'(-1) - 5\ln 2 - 3$	0.0666
W	$\sum_{n=2}^{\infty} \frac{1}{n} \ln \left[\frac{(4n^2-1)^2}{16n^2(n^2-1)} \right]$	0.1205
W_{00}	$-2\gamma_E + 24\zeta'(-1) + (17/3)\ln 2 + 2\ln 3 + W$	1.1210
W_{01}	$-3\ln 2 + 2\ln 3 + W$	0.2383
W_{11}	$-24\zeta'(-1) - (35/3)\ln 2 + 2\ln 3 + 2 + W$	0.2011

TABLE II. Power counting rules in the kinematic region appropriate for studying screening states at high T .

ϵ_B	K	\mathbf{P}	ψ	$i\partial_t$	$i\partial$	$g_3\mathcal{A}_0$	$g_3\mathcal{A}$	$g_3\varphi$	$g_3\mathcal{E}$	$g_3\mathcal{B}$
g^2T	g^2T	gT	gT	g^2T	gT	g^2T	g^3T	g^2T	g^3T^2	g^4T^2

TABLE III. Coefficients of the one-loop corrections.

coefficient	analytic expression	numerical value
c_1	$C_f[c - 3 + (X + X_{11} - iX_{10})/2]$	$C_f[c - 2.6768]$
c_2	$C_f[c - (3 - X + X_{00} + iX_{10})/2]$	$C_f[c - 2.0551]$
c_3	$C_f[c + (Y + Y_{11} - iY_{10})/2] + C_{ad}[c - 1]$	$C_f[c + 0.3232] + C_{ad}[c - 1]$
c_4	$C_f[c + (Y + Y_{00} + iY_{01})/2]$	$C_f[c + 1.3232]$
	$+C_{ad}[c - (Y + Y_{00} + iY_{01})/4 + (Z + Z_{00} + iZ_{01})/2]$	$+C_{ad}[c - 0.3232]$

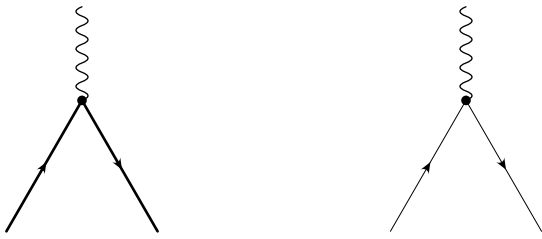


Figure 1

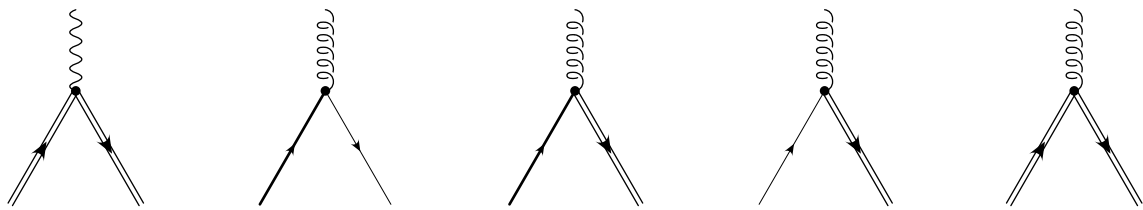
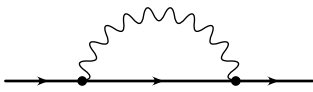
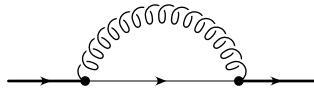


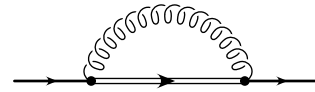
Figure 2



(a)

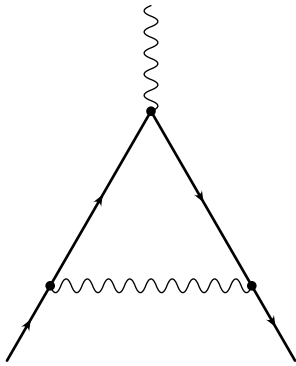


(b)

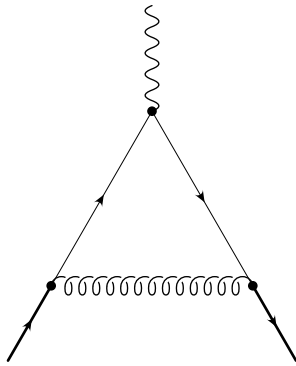


(c)

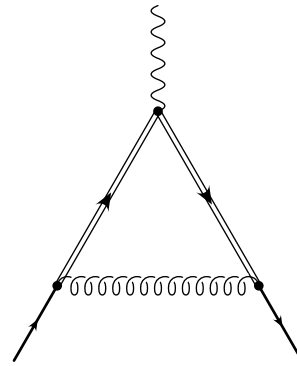
Figure 3



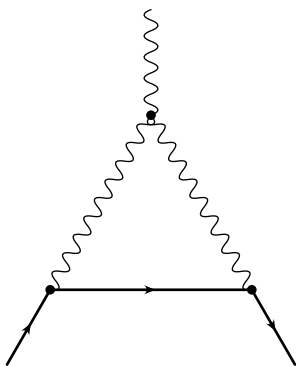
(a)



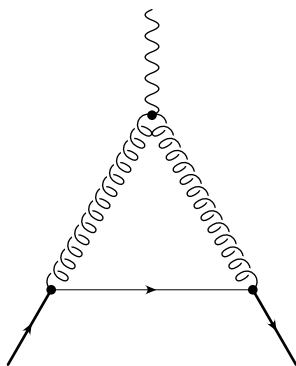
(b)



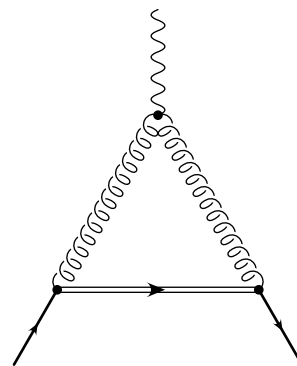
(c)



(d)

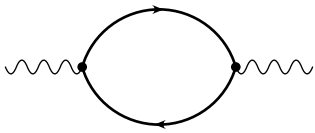


(e)

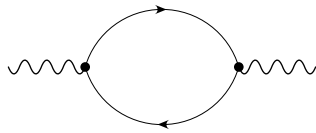


(f)

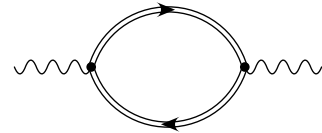
Figure 4



(a)

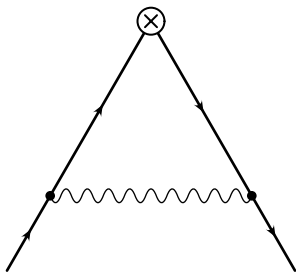


(b)

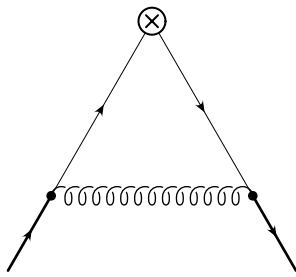


(c)

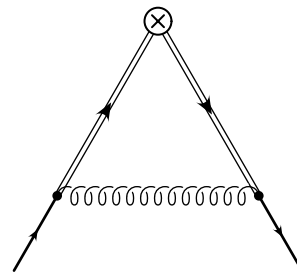
Figure 5



(a)



(b)



(c)

Figure 6



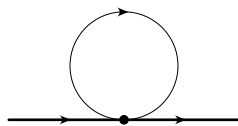
(a)



(b)



(c)



(d)

Figure 7